IEEE Access
Multidisciplinary | Rapid Review | Open Access Journal

Received 17 November 2022, accepted 10 December 2022, date of publication 12 December 2022,
date of current version 16 December 2022.

Digital Object Identifier 10.1109/ACCESS.2022.3228837

RESEARCH ARTICLE

Device-Free Localization Using Enhanced Channel Selection and a Distance-Based Elliptical Model

GUOPING LI AND QIAN LEI
School of Electrical and Information Engineering, Wuhan Institute of Technology, Wuhan 430074, China
Corresponding author: Qian Lei (leiqian_0521@whu.edu.cn)

This work was supported in part by the Scientific Research Project of Education Department of Hubei Province under Grant B2021079, and in part by the Research Project of Wuhan Institute of Technology under Grant 20QD14.

ABSTRACT Device-free localization (DFL) based on wireless sensor networks (WSNs) is a technology that can detect and locate a person by measuring the changes in received signals without the need for any wireless devices. As an emerging important technology in WSNs, radio tomographic imaging (RTI) has received increasing attention. However, there is much room to improve localization accuracy in RTI. To address this issue, an enhanced channel-selection method and a new distance-based elliptical model are proposed to improve the localization accuracy. The enhanced frequency channel-selection method selects two channels with the lowest received signal strength (RSS) variances to collect data. This approach is more robust to environmental change. The new distance-based elliptical model is based on the distance between the voxels and sensors. Meanwhile, the communication links are divided into line-of-sight (LOS) paths and nonline-of-sight (NLOS) paths. Experimental results demonstrate that the proposed algorithm improves the accuracy of positioning by up to 44.8% over some state-of-the-art RTI methods with low cost.

INDEX TERMS Device-free localization, wireless sensor networks, received signal strength, radio tomographic imaging, elliptical model.

I. INTRODUCTION

Device-free localization (DFL) is a technology for detecting and tracking a human in indoor and outdoor environments without the need for any wireless devices in wireless sensor networks (WSNs) [1], [2], [3]. DFL has attracted a great deal of research attention in security and monitoring systems for indoor and outdoor areas, e.g., emergency rescue systems, security monitoring systems and health care systems [4], [5], [6], [7].

There are three main measuring techniques: (1) technologies on narrowband (NB) [8], [9], (2) ultrawideband (UWB) [10], [11], [12] and (3) received signal strength (RSS) [13], [14], [15], [16]. In particular, NB-based DFL technology is used to detect the moving objects by measuring the sum of the contributions of all multipaths. However, narrowband receivers cannot provide the individual multipath information, and localization via signal delay is very difficult [8], [9]. In [10], UWB-based DFL technology has the advantages of a high data rate, and high positioning accuracy by utilizing a nanosecond pulse to deliver information, and the high memory and computing resources for accurate localization performance are needed. Compared with NB and UWB technologies, RSS-based DFL can be used to locate a person with low cost and low power consumption.

There are five Classical algorithms extensively used in DFL systems, e.g., the fingerprint (FP) [17], [18], [19], [20], radio tomographic imaging (RTI) [1], [15], [21], [22], [23], [24], the support vector machine (SVM) [25], [26], [27], the Bayesian system [16], [28], [29], and compressed sensing (CS) [30], [31], [32]. Algorithms studied in the literature are presented, as summarized in Table 1. Among the above techniques, RSS-based RTI systems have been widely investigated in recent years due to low power consumption and cost.

As for RTI, the authors in [1] proposed the RTI system by measuring shadowing losses on links between pairs of nodes in WSNs for the first time, and the RSS on many

The associate editor coordinating the review of this manuscript and approving it for publication was Chun-Wei Tsai.

TABLE 1. Algorithms, literatures, measurements and position dependence.

Algorithm	Literature	Measurement	Position dependence
Ultra-Narrowband	[8], [9]	Narrowband	Relative
Ultra-Wideband	[10], [11], [12]	UWB	Relative
Localization from RSS	[4], [5], [6], [7], [13], [14], [15], [16]	RSS	Absolute
Fingerprint-Matching	[3], [17], [18], [19], [20]	RSS	Absolute
Radio Tomographic Imaging	[1], [2], [15], [21], [22], [23], [24], [33]	RSS	Absolute
Support Vector Machine	[25], [26], [27]	RSS	Absolute
Bayesian system	[16], [28], [29]	RSS	Relative
Compressed Sensing	[30], [31], [32]	RSS	Relative

different paths was measured through a medium to derive an image estimator. The communication links were mathematically described as elliptical weight models with a Gaussian image prior. The monitoring area was divided into voxels. The weightings of voxels inside one elliptical weight mode were the same, which was not consistent with the actual situation. Consequently, several researchers studied the elliptical weight model for improvement in localization estimation accuracy in RTI. A linear mixed elliptical model was proposed in [21], and LOS-only signal strength was measured. In other words, the voxels along the direct NLOS between transmitter and receiver nodes received zero weight. A novel outdoor RTI method was proposed in [22], where the RSS signal was time-variant, e.g., due to rainfall or wind-driven foliage. The sensitivity area of the ellipse was expressed as the component of the elliptical weight model. Authors in [33] divided the communication link into LOS path and NLOS paths, and the localization accuracy was improved. To adaptively select the voxel weightings, a distance attenuation-based elliptical weight model was proposed in [23], which was based on the distance between each voxel inside the ellipse and the LOS path. However, the distance between voxels and sensor nodes was not studied, which is not consistent with the actual situation. Meanwhile, the localization accuracy could be further improved.

In this paper, we focus on improving the localization accuracy in RTI. For this purpose, an enhanced channel-selection method and a new distance-based elliptical model are proposed. Based on the data provided by Neal Patwari [1], in the data-collecting procedure, two links with the highest average RSS are selected, which is robust to environmental change [3]. The RSS variances of all channels on the two links are computed. One channel with the lowest RSS variance on one link is selected, and two channels with the lowest RSS variances are selected. For the new distance-based elliptical model, LOS and NLOS path information are used to locate a person. The distance between each voxel and sensors is smaller, and the weight of the elliptical model is higher.

In addition, most DFL schemes require high memory and computing resources for accurate tracking performance, and thus may not be suitable for resource-constrained applications. The proposed elliptical weighting model only focus on the distance between voxels and sensor nodes, which would reduces the algorithm's storage and computational resource requirements resulting in fast execution times.

The main contributions of this paper are summarized as follows:

1) An enhanced channel-selection method is proposed. The data selected from the two links with the highest average RSS is robust to environmental change [3]. In addition, the data with the lowest RSS variance would contribute to the detection and localization problems [22]. Only two channels are utilized to collect data, and the complexity of this method is low.

2) A new distance-based elliptical model is proposed. We prove that the smaller the voxel's distance to the sensor node is, and the larger the value of the distance-based weight should be. Voxels that are closer to the sensor node are assigned higher weights compared to other voxels, which improves the localization accuracy.

The rest of this paper is organized as follows. Section II discusses the data-collecting method, which consists of link-channel pair selection and enhanced channel selection. In Section III, the distance-based elliptical model is introduced. Experimental results are presented in Section IV. Finally, Section V draws conclusions.

II. DATA-COLLECTING METHOD

As shown in Fig. 1, there are N sensor nodes in the monitoring area, and each sensor node is assigned a number from the sequence $1, 2, 3, \ldots, N$. The communication link is set up by any two sensor nodes that can communicate directly. Consequently, there are C_N^2 links in this monitoring area. The experimental data r can be described as:

$$r = [RSS_{1,1}, \ldots, RSS_{1,C}, \ldots, RSS_{l,c}, \ldots, RSS_{L,C}]^T, \quad (1)$$

where l is the index of communication links, $l = 1, 2, 3, \ldots, L, L \in N_+$; c is the index of frequency channels; C is the number of frequency channels, $c = 1, 2, 3, \ldots, C, C \in N_+$; and T represents the transpose of a given matrix. When a person enters a network area, some transmitted power is absorbed, reflected, or diffracted, which creates shadowing losses [1]. The received signal strength can be mathematically described as:

$$y_l = P_l - L_l - S_l - n_l, \quad (2)$$

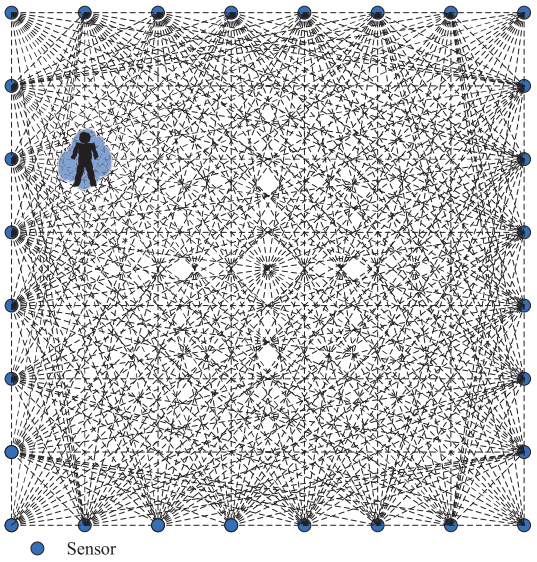

FIGURE 1. The display of sensors in the DFL system.

where P_l represents transmit power; L_l is the static losses due to the distance, antenna patterns, device inconsistencies, etc; S_l represents shadowing loss, which be approximated as a sum of attenuation that occurs in each voxel; and n_l is the noise.

A. LINK-CHANNEL PAIR SELECTION

Avoiding the negative influence of the shadowing losses is an alternative way of improving localization accuracy. To address this issue, several researchers have focused on the improvement of data-collecting methods. In [22], the authors proposed a link-channel pair selection method, which selects one link-channel pair with the lowest RSS variance to collect data. First, the average RSS of all link-channel pairs are computed, and the link-channel pairs with highly average RSS are selected. Then, RSS variances of the link-channel pairs selected are computed, and the link-channel pair with the lowest RSS variance is selected, which is shown in Fig. 2. The data with a higher RSS variance would be in deep fade, which would hardly contribute to the detection and localization problems.

B. ENHANCED CHANNEL SELECTION

The data with the lowest RSS variance is robust to the environmental change, so it can achieve better localization accuracy [22]. However, only one link-channel pair is selected. When the environment changes markedly, the selected channel is not sufficient enough to improve of the localization accuracy.

In this paper, we propose an enhanced channel-selection method. First, the average RSS of all communication links is computed. The highest two links are selected, and the complexity is $\mathcal{O}(L)$. The link with the highest average RSS is more robust to the environmental change [3]. Second, all channels on those two communication links are sorted by the RSS variances. Then, one channel with the lowest RSS variance on one link is selected, i.e., two channels from the two links are selected (shown in Fig. 2 and *Algorithm* 1), and the complexity is $\mathcal{O}(C)$. Compared with the method in [22], the complexity is not increased, and the proposed channel-selection method will be more rubust for the environment change.

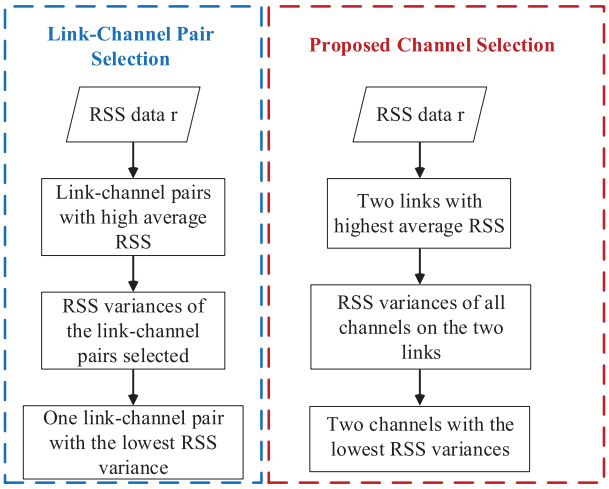

FIGURE 2. The comparison between the link-channel pair selection method [22] and the proposed channel-selection method.

Algorithm 1 The Proposed Channel-Selection Method

Input: The RSS data r.
Output: Two channels with the lowest RSS variance.
for the data $r = [RSS_{1,1}, \ldots, RSS_{1,C}, \ldots, RSS_{l,c}, \ldots, RSS_{L,C}]^T$ **do**
  Compute the average RSS of each link on all frequency channels.
  if $AverageRSS_{l_1} = max[AverageRSS_1, \ldots, AverageRSS_L]$, $1 \leqslant l_1 \leqslant L$ **then**
    Select the link l_1.
    Compute the RSS variance (σ) [22] of the link l_1 on all frequency channels.
    if $\left\{\sigma_{c_1}^{l_1}, \sigma_{c_2}^{l_1}\right\} = min[\sigma_1^{l_1}, \sigma_2^{l_1}, \ldots, \sigma_C^{l_1}]$ **then**
      Select the two channels c_1 and c_2, $1 \leq c_1 \leq C$, $1 \leq c_2 \leq C$.
    end if
  end if
end for

III. DISTANCE-BASED ELLIPTICAL MODEL

After the data is collected from the two channels based on the proposed channel-selecting method, the challenge is then to increase localization performance. In [23], the monitoring area was divided into voxels. An elliptical weighting model representing the communication link was proposed in RTI that adaptively selected the voxel weightings. However, the localization accuracy could be further improved. In this paper, a new distance-based elliptical model in RTI systems is proposed.

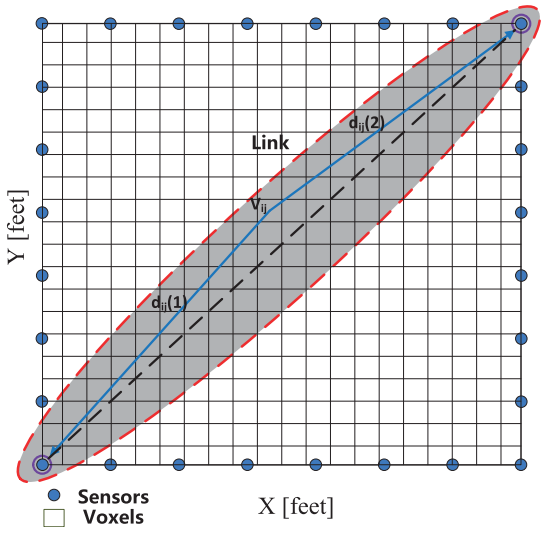

FIGURE 3. Elliptical weighting model in the RTI system.

A. RADIO TOMOGRAPHY IMAGING

When a person within the area absorbs, reflects, diffracts, or scatters some of the transmitted power, shadowing losses are created. Meanwhile, the attenuation of different links is used by RTI algorithms to locate a person without the need for any physical devices, e.g., sensors or tags [1].

As shown in Fig. 3, there are N sensors in the RTI system. The monitoring area is divided into voxels, whose dimensions are $I \times J$. Each communication link is expressed as an ellipse [1]. Because the contribution of each voxel to the attenuation of a link is different for each link and all static losses can be removed over time, the RTI system is described in the following:

$$\Delta y_l = y_l - \bar{y_l} = \sum_{i=1}^{I}\sum_{j=1}^{J} W_{ij}^l \Delta x_{ij} + n_l, \tag{3}$$

where l is the index of links; L is the number of links, $l = C_N^2 = 1, 2, 3, \ldots, L, L \in N_+$; Δy_l is the change in signal power in link l; and i and j are the indices of voxels in RTI systems, $i = 1, 2, 3, \ldots, I, j = 1, 2, 3, \ldots, J, I \in N_+, J \in N_+$; $\bar{y_l}$ is the average value of the Δy_l; W_{ij}^l is the weighting of voxel V_{ij} in link l; Δx_{ij} is the attenuation change of voxel V_{ij}; and n_l is the noise of link l. Formula (1) can be described in matrix form:

$$\Delta \mathbf{y} = \mathbf{W}\Delta \mathbf{x} + \mathbf{n}, \tag{4}$$

where $\Delta \mathbf{y}$, $\Delta \mathbf{x}$, $\mathbf{n}$ and $\mathbf{W}$ can be defined in the following relationships [1]:

$$\Delta \mathbf{y} = [\Delta y_1, \Delta y_2, \ldots, \Delta y_L]^T, \tag{5}$$

$$\mathbf{W} = \begin{bmatrix} W_{11} & W_{12} & \ldots & W_{1(I\times J)} \\ W_{21} & W_{22} & \ldots & W_{2(I\times J)} \\ \ldots & \ldots & \ldots & \ldots \\ W_{L1} & W_{L2} & \ldots & W_{L(I\times J)} \end{bmatrix}, \tag{6}$$

$$\Delta \mathbf{x} = [\Delta x_1, \Delta x_2, \ldots, \Delta x_{I\times J}]^T, \tag{7}$$

$$\mathbf{n} = [n_1, n_2, \ldots, n_L]^T, \tag{8}$$

where $\Delta \mathbf{y}$ is the variation in RSS of all links; $\mathbf{W}$ is the weighting model vector; $\Delta \mathbf{x}$ is the attenuation of all voxels; $\mathbf{n}$ is the noise vector; $I \times J$ is the number of voxels in the network, $I \in N_+, J \in N_+$; and T represents the transpose of a given matrix.

B. DISTANCE-BASED ELLIPTICAL MODEL

To distinguish the difference in path loss in RTI systems, the authors in [23] proposed an attenuation-based elliptical model, which focused on the distance between each voxel inside the ellipse and the LOS path. The weighting is described as follows:

$$W_{ij}^l = \begin{cases} e^{-h} & \text{if } d_{ij}^l(1) + d_{ij}^l(2) < d + \lambda \\ 0 & otherwise, \end{cases} \tag{9}$$

where h represents the distance between the LOS path and each voxel inside the ellipse; d is the length of link l; λ is a parameter that determines the range of the ellipse; and $d_{i,j}^l(1)$ and $d_{i,j}^l(2)$ are the distances between voxel V_{ij} and the sensor nodes. The proposed ellipse model adaptively selects the voxel weightings, and the difference in path loss in the target area is determined [23] (shown in Fig. 4(a) and Fig. 4(b)). In addition, compared with the algorithm in [1], the localization accuracy is improved.

However, the distance between voxels and sensor nodes is not taken into consideration, which is not consistent with a real-world situation. In practice, the distance between a person and sensors is smaller, and the interruption of the signal is greater.

In this paper, a new distance-based elliptical model is proposed. The new weighting model can be mathematically described as:

$$W_{ij}^l = \begin{cases} e^{-min\left\{d_{ij}^l(1), d_{ij}^l(2)\right\}} & \text{if } d_{ij}^l(1) + d_{ij}^l(2) < d + \lambda \\ 0 & otherwise. \end{cases} \tag{10}$$

The voxels closer to the sensor nodes should be assigned a higher weight. In addition, the voxel in the LOS path has a higher weight than the voxels nearby in the NLOS path. Compared with the model in [23], $e^{-min\left\{d_{ij}^l(1), d_{ij}^l(2)\right\}}$ refines each voxel weighting. In addition, compared with the method in [33], the ellipse can be divided in a more realistic way by using the proposed method. However, the complexity is increased due to the addition of the enhanced channel-selection method. As shown in Fig. 4(c) and Fig. 4(d), the voxels' weightings near the sensor nodes are higher, which is more in line with reality.

C. IMAGE RECONSTRUCTION

In Formula (4), the weighting matrix $\mathbf{W}$ is underdetermined, i.e., the same set of experiments could lead to multiple different images [1]. Hence, the $\Delta \mathbf{x}$ estimated in Formula (4) is

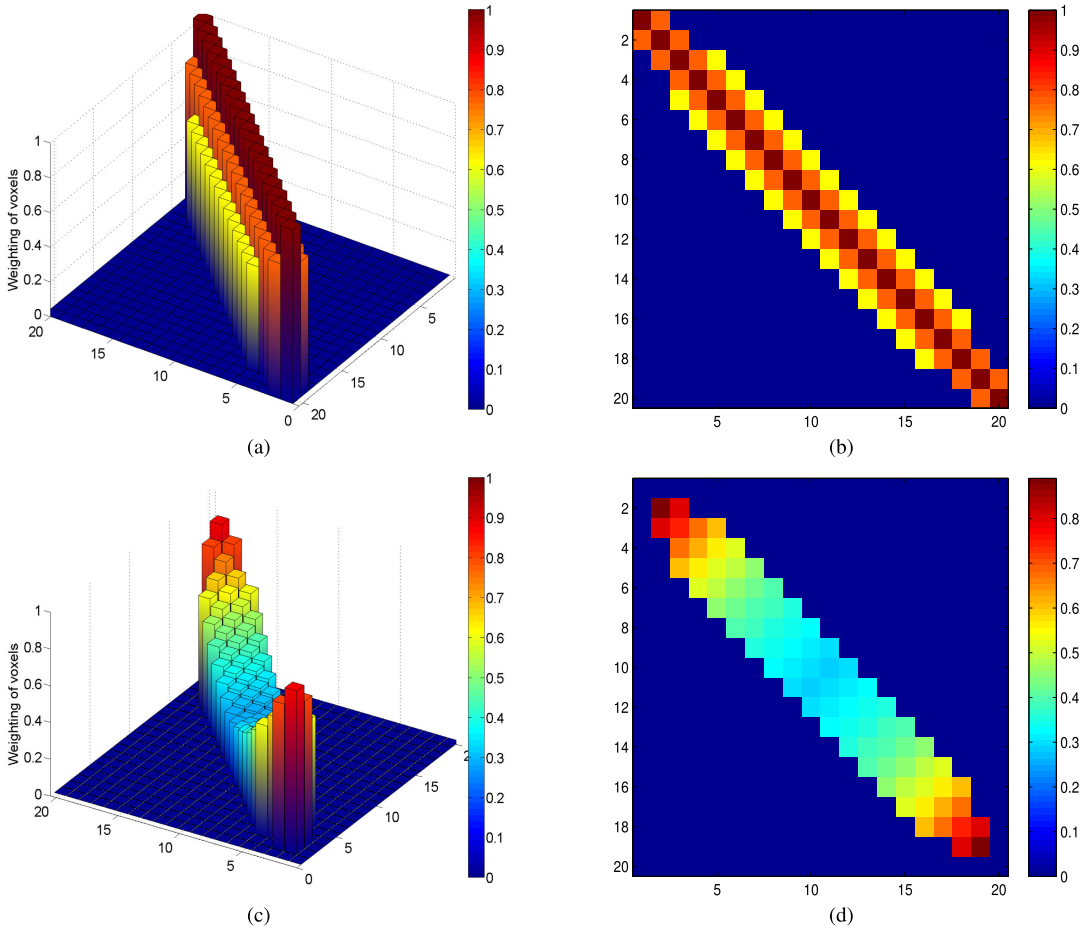

FIGURE 4. (a) The 3D weighting elliptical model in [23]; (b) The 2D weighting elliptical model in [23]; (c) The 3D proposed weighting elliptical model; (d) The 2D proposed weighting elliptical model.

FIGURE 5. Photograph of the deployed network.

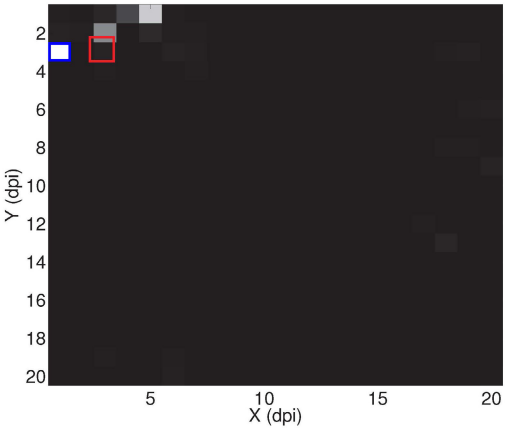

FIGURE 6. The difference between the actual position (red rectangle) and the estimated position (white voxel with blue rectangle).

not unique, and is considered as an ill-posed inverse problem. In [1], Tikhonov regularization was utilized. It is described in the following:

$$f(x) = \frac{1}{2}\|\mathbf{W}\Delta\mathbf{x} - \Delta\mathbf{y}\|^2 + \alpha(\|\mathbf{D_x}x\|^2 + \|\mathbf{D_y}x\|^2), \quad (11)$$

$$\Delta\mathbf{x} = (\mathbf{W}^T\mathbf{W} + \alpha(\mathbf{D_x}^T\mathbf{D_x} + \mathbf{D_y}^T\mathbf{D_y}))^{-1}\mathbf{W}^T, \quad (12)$$

where $\mathbf{D_x}$ is the operator for the horizontal direction; $\mathbf{D_y}$ is the operator for the vertical direction; α is the weighting parameter; and $f(x)$ represents the objective function. By utilizing

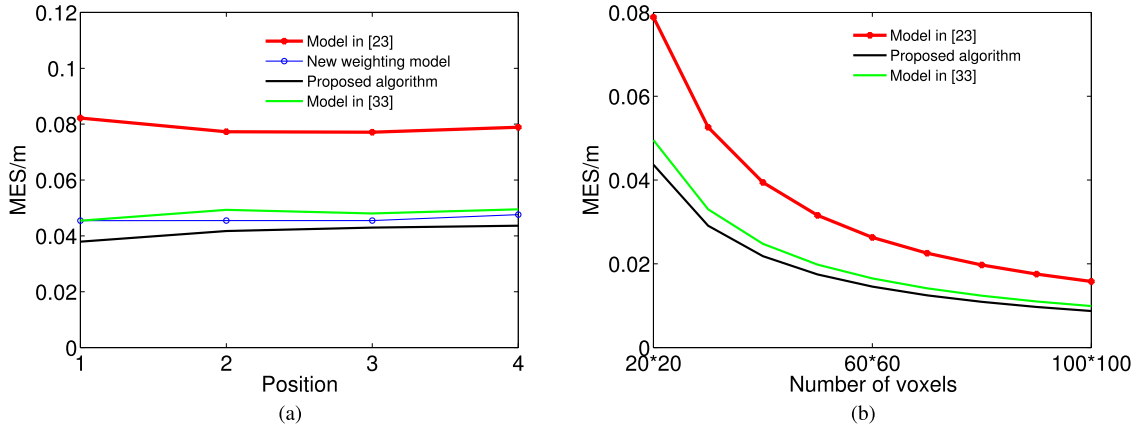

FIGURE 7. (a) The experimental result for the localization of one person. (b) As the number of voxels increases, the contrast between the two algorithms for the localization.

the Tikhonov regularization, the unique position estimated is achieved.

IV. EXPERIMENTAL RESULTS

The measured data of the experiment are the same as in [1], and the experiment was conducted at the University of Utah. As shown in Fig. 5, the monitoring area is 21 × 21 foot square, and 28 sensor nodes around that. Two trees are in the deployed network so that static objects exist in the tested RTI system, which absorbs, diffracts, reflects, or scatters some of the power of the electromagnetic waves [1]. Each wireless sensor node operates in the 2.4 GHz frequency band for communication, utilizing the IEEE 802.15.4 communication standard. In the experiment, each node is assigned an ID number and programmed, and all network traffic is listened by a base station node. When a node transmits, each node that receives the transmission examines the sender identification number. Since the base station node is within range of all nodes, the latency of measurement retrieval to the laptop is low, on the order of a few milliseconds.

The mean-squared error (MSE) ϵ of the normalized image can be defined as:

$$\epsilon = \frac{\left\| x_{real} - \hat{x}_{I\times J} \right\|^2}{I \times J}, \tag{13}$$

where $I \times J$ is the number of voxels in the monitoring sensor area; $\mathbf{x_{real}}$ is the actual position for a human; and $\hat{x}_{I\times J}$ is the estimated position. When a person enters the deployed network, there is more noise, which comes from fading loss, shadowing loss, and measurement noise in the experiment,all of which affect the localization accuracy [1].

As shown in Fig. 6, the bright spots represent the estimated positions, the white voxel with a blue rectangle represents the position estimated by the proposed algorithm, and the red rectangle represents the actual position. Compared with the methods in [1] and [23], many extra bright spots in image reconstruction are eliminated, which decreases the difficulty of localization. The extra bright spots could come from fading loss, shadowing loss, and measurement noise in the experiment, which affected localization accuracy [1]. Method in [22] only select one link-channel pair to collect experiment data. When the environment changes from time to time, the localization accuracy will be affected. Compared with the method in [22], two channels are selected in proposed channel-selection method, which would be more rubust to the environment change.

In Fig. 7(a), the vertical axis represents the average of the MSE in position estimation, the horizontal axis shows the position numbers for one person, the red line represents the experimental results by using the method in [23], the blue line represents the effect of the new weighting model when the image reconstruction method is the same as in [23], the green line represents the function of the method in [33], and the black line represents the effect of the new weighting model by using the enhanced channel-selection method in localization estimation.

Compared with the method in [23], utilizing the new weighting model improves the positioning accuracy by up to 39.7%, and the proposed algorithm in this paper improves the localization accuracy by up to 44.8%. As the number of positions increases, more noise that would come from fading loss, shadowing loss, and measurement noise in the experiment could affect localization accuracy. The proposed channel-selection method would be more rubust to the environment change than the method in [23], and the localization accuracy is improved. In addition, the proposed weighting model takes the distances between the voxels and the sensor nodes into consideration, which would be more in accordance with reality. Compared with the method in [33], the complexity of the proposed algorithm is increased own to the addition of the channel-selection method, and the localization accuracy is further improved.

In Fig. 7(b), the vertical axis shows the MSE in position estimation, the horizontal axis shows the number of voxels in the monitoring area, the red line displays the experiment results in [23], the green line displays the effect of the

method in [33], and the black line displays the function of the proposed algorithm. As the number of voxels increases, the MSE in the three algorithms decreases. The reason is that the complexity of the three algorithms would increase, which would improve the localization accuracy. Then, the MSE in the three algorithms tends toward stability because of the more noise coming from fading loss, shadowing loss, and measurement noise in the experiment. Compared with the method in [23], the proposed algorithm achieves a better localization effect by up to 44.6% by using proposed channel-selection method and the new distance-based elliptical model. Compared with the method in [33], the proposed algorithm achieves a better localization effect by up to 11.8% own to the proposed channel-selection method, which would be more rubust to the environment change.

V. CONCLUSION

In this paper, we propose an enhanced channel-selection method and a new distance-based elliptical model in RTI. The enhanced channel-selection method selects two channels with the lowest RSS variances to collect data. This approach is more robust to environmental change. By using the new distance-based elliptical model, localization accuracy is improved. Experimental results are presented to confirm the performance improvement.

However, compared with the method in [23], the complexity of the proposed method is increased to ensure the localization improvement. Meanwhile, this paper focus on the viability of the proposed algorithm, and the network was placed in an outdoor environment. When in an indoor environment, the electromagnetic environment will be more complex. The objects within the monitoring area will absorb, reflect, diffract, or scatter some of the transmitted power.

In the future, on the one hand the proposed scheme for two or more persons in dense signal environment will be investigated. On the other hand, efficient elliptical model in RTI will be explored.

ACKNOWLEDGMENT

This work is based on data provided by Neal Patwari, and the authors are grateful for his enthusiastic help. The authors declare that they have no conflicts of interest to report regarding the present study.

REFERENCES

[1] J. Wilson and N. Patwari, "Radio tomographic imaging with wireless networks," *IEEE Trans. Mobile Comput.*, vol. 9, no. 5, pp. 621–632, May 2010.

[2] N. Patwari and J. Wilson, "RF sensor networks for device-free localization: Measurements, models, and algorithms," *Proc. IEEE*, vol. 98, no. 11, pp. 1961–1973, Nov. 2010.

[3] Q. Lei, H. Zhang, H. Sun, and L. Tang, "Fingerprint-based device-free localization in changing environments using enhanced channel selection and logistic regression," *IEEE Access*, vol. 6, pp. 2569–2577, 2018.

[4] J. Yan, L. Wan, W. Wei, X. Wu, W.-P. Zhu, and D. P.-K. Lun, "Device-free activity detection and wireless localization based on CNN using channel state information measurement," *IEEE Sensors J.*, vol. 21, no. 21, pp. 24482–24494, Nov. 2021.

[5] F. Alam, N. Faulkner, and B. Parr, "Device-free localization: A review of non-RF techniques for unobtrusive indoor positioning," *IEEE Internet Things J.*, vol. 8, no. 6, pp. 4228–4249, Mar. 2021.

[6] N. Faulkner, F. Alam, M. Legg, and S. Demidenko, "Device-free localization using privacy-preserving infrared signatures acquired from thermopiles and machine learning," *IEEE Access*, vol. 9, pp. 81786–81797, 2021.

[7] Z. Wu, X. Pan, K. Fan, K. Liu, and Y. Xiang, "Device-free orientation detection based on CSI and visibility graph," *IEEE Trans. Syst., Man, Cybern. Syst.*, vol. 51, no. 7, pp. 4433–4442, Jul. 2021.

[8] J. Ninnemann, P. Schwarzbach, A. Jung, and O. Michler, "Device-free passive localization based on narrowband channel impulse responses," in *Proc. 21st Int. Radar Symp. (IRS)*, Oct. 2020, pp. 88–93.

[9] J. Wilson and N. Patwari, "A fade-level skew-Laplace signal strength model for device-free localization with wireless networks," *IEEE Trans. Mobile Comput.*, vol. 11, no. 6, pp. 947–958, Jun. 2012.

[10] J. Yang, M. Wang, Y. Yang, and J. Wang, "A device-free localization and size prediction system for road vehicle surveillance via UWB networks," *IEEE Trans. Instrum. Meas.*, vol. 71, pp. 1–11, 2022.

[11] M. Cimdins, S. O. Schmidt, and H. Hellbruck, "Comparison of I/Q- and magnitude-based UWB channel impulse responses for device-free localization," in *Proc. Int. Conf. Localization GNSS (ICL-GNSS)*, Jun. 2021, pp. 1–7.

[12] K. Bregar, A. Hrovat, M. Mohorcic, and T. Javornik, "Self-calibrated UWB based device-free indoor localization and activity detection approach," in *Proc. Eur. Conf. Netw. Commun. (EuCNC)*, Jun. 2020, pp. 176–181.

[13] Y. Ma, W. Ning, and B. Wang, "Training-free artifact detection method for radio tomographic imaging based device-free localization," *IEEE Trans. Veh. Technol.*, vol. 70, no. 10, pp. 10382–10394, Oct. 2021.

[14] P. Hillyard and N. Patwari, "Never use labels: Signal strength-based Bayesian device-free localization in changing environments," *IEEE Trans. Mobile Comput.*, vol. 19, no. 4, pp. 894–906, Apr. 2020.

[15] X. Ding, T.-M. Choi, and Y. Tian, "HRI: Hierarchic radio imaging-based device-free localization," *IEEE Trans. Syst., Man, Cybern. Syst.*, vol. 52, no. 1, pp. 287–300, Jan. 2022.

[16] O. Kaltiokallio, R. Hostettler, and N. Patwari, "A novel Bayesian filter for RSS-based device-free localization and tracking," *IEEE Trans. Mobile Comput.*, vol. 20, no. 3, pp. 780–795, Mar. 2021.

[17] S. Zhang, K. Liu, Y. Zhang, and Y. Wang, "A coarse fingerprint-assisted multiple target indoor device-free localization with visible light sensing," *IEEE Sensors J.*, vol. 22, no. 2, pp. 1461–1473, Nov. 2021.

[18] M. Chen, K. Liu, J. Ma, X. Zeng, Z. Dong, G. Tong, and C. Liu, "MOLOC: Unsupervised fingerprint roaming for device-free indoor localization in a mobile ship environment," *IEEE Internet Things J.*, vol. 7, no. 12, pp. 11851–11862, Dec. 2020.

[19] W. Wei, J. Yan, X. Wu, C. Wang, and G. Zhang, "CSI fingerprinting for device-free localization: Phase calibration and SSIM-based augmentation," *IEEE Wireless Commun. Lett.*, vol. 11, no. 6, pp. 1137–1141, Jun. 2022.

[20] K. M. Chen, R. Y. Chang, and S.-J. Liu, "Interpreting convolutional neural networks for device-free Wi-Fi fingerprinting indoor localization via information visualization," *IEEE Access*, vol. 7, pp. 172156–172166, 2019.

[21] B. Beck, X. Ma, and R. Baxley, "Ultrawideband tomographic imaging in uncalibrated networks," *IEEE Trans. Wireless Commun.*, vol. 15, no. 9, pp. 6474–6486, Sep. 2016.

[22] C. Alippi, M. Bocca, G. Boracchi, N. Patwari, and M. Roveri, "*RTI Goes Wild*: Radio tomographic imaging for outdoor people detection and localization," *IEEE Trans. Mobile Comput.*, vol. 15, no. 10, pp. 2585–2598, Oct. 2014.

[23] C. Zhu and Y. Chen, "Distance attenuation-based elliptical weighting-g model in radio tomography imaging," *IEEE Access*, vol. 6, pp. 34691–34695, 2018.

[24] X. Zhang, Y. Ma, X. Gong, H. Fu, B. Wang, W. Ning, and X. Liang, "A training-free multipath enhancement (TFME-RTI) method for device-free multi-target localization," *IEEE Sensors J.*, vol. 22, no. 7, pp. 7399–7410, Apr. 2022.

[25] R. Zhou, X. Lu, P. Zhao, and J. Chen, "Device-free presence detection and localization with SVM and CSI fingerprinting," *IEEE Sensors J.*, vol. 17, no. 23, pp. 7990–7999, Dec. 2017.

[26] J. Hong and T. Ohtsuki, "Signal eigenvector-based device-free passive localization using array sensor," *IEEE Trans. Veh. Technol.*, vol. 64, no. 4, pp. 1354–1363, Apr. 2015.

[27] R. Zhou, J. Chen, X. Lu, and J. Wu, "CSI fingerprinting with SVM regression to achieve device-free passive localization," in *Proc. IEEE 18th Int. Symp. A World Wireless, Mobile Multimedia Netw. (WoWMoM)*, Jun. 2017, pp. 1–9.
[28] M. Schmidhammer, B. Siebler, C. Gentner, S. Sand, and U.-C. Fiebig, "Bayesian approaches to multipath-enhanced device-free localization," in *Proc. 15th Eur. Conf. Antennas Propag. (EuCAP)*, Mar. 2021, pp. 1–5.
[29] J. Tan, X. Zhao, X. Guo, and G. Wang, "Exploring the spatial correlation of shadowing in RF-based device-free localization by block sparse Bayesian learning," in *Proc. IEEE Int. Conf. Robot. Biomimetics (ROBIO)*, Dec. 2021, pp. 1786–1791.
[30] Y. Guo, S. Yang, N. Li, and X. Jiang, "Device-free localization scheme with time-varying gestures using block compressive sensing," *IEEE Access*, vol. 8, pp. 88951–88960, 2020.
[31] S. Yang, Y. Guo, N. Li, and P. Qian, "Compressive sensing based device-free multi-target localization using quantized measurement," *IEEE Access*, vol. 7, pp. 73172–73181, 2019.
[32] L. Zhao, H. Huang, C. Su, S. Ding, H. Huang, Z. Tan, and Z. Li, "Block-sparse coding-based machine learning approach for dependable device-free localization in IoT environment," *IEEE Internet Things J.*, vol. 8, no. 5, pp. 3211–3223, Mar. 2021.
[33] Q. Lei, H. Zhang, H. Sun, and L. Tang, "A new elliptical model for device-free localization," *Sensors*, vol. 16, no. 4, p. 577, 2016.

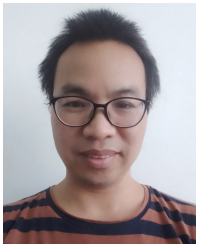

GUOPING LI was born in China, in 1978. He received the M.S. degree from the School of Mechanical and Electronic Engineering, Wuhan University of Technology, China, in 2005. He joined the School of Electrical and Information Engineering, Wuhan Institute of Technology, as an Instructor, in 2005, and subsequently became an Assistant Professor. His research interests include signal processing, device-free localization, and embedded systems.

QIAN LEI was born in China, in 1987. He received the Ph.D. degree from the School of Electronic Information, Wuhan University, China, in 2018. He joined the School of Electrical and Information Engineering, Wuhan Institute of Technology, as an Instructor, in 2019, and subsequently became an Assistant Professor. His research interests include device-free localization, signal processing, and android.